3D virtual reconstruction of the Pleistocene cheetah skull from the Tangshan, Nanjing, China*

DONG Wei[1,2**], HOU Xinwen[2], LIU Jinyi[1], FANG Yingsan[3], JIN Changzhu[1] and ZHU Qizhi[4]

(1. Institute of Vertebrate Paleontology and Paleoanthropology, Chinese Academy of Sciences, Beijing 100044, China; 2. State Key Laboratory of Pattern Recognition, Institute of Automation, Chinese Academy of Sciences, Beijing 100080, China; 3. Nanjing Provincial Museum, Nanjing 210016, China; 4. Radiology Department, Renmin Hospital, Peking University, Beijing 100044, China)

Accepted on May 30, 2006

Abstract The development of computer tomography and image processing has made it possible to establish virtual 3D reconstruction and non-invasive dissection of fossil specimens. We used these methods to reconstruct a virtual 3D skull of a Pleistocene cheetah skull from the Tuozi cave, Tangshan, Nanjing, and virtually dissected it for anatomic studies, and measured the volumes of different parts of the endocranium. The endocranium of the cheetah skull has showed that its frontal sinus is beehive-like, the frontal lobe of cerebra is relatively large but the temporal lobe is relatively small, its cerebral sulcus and gyrus are more complicated than those of the domestic cat, similar to those of the domestic dog, but simpler than those of giant panda, pig, cattle and horse. The technology of virtual 3D reconstruction and non-invasive dissection of fossil specimens can extend the morphological study from the exterior to the interior, and it can also help to study fragile specimens and virtually backup rare and precious specimens.

Keywords: CT imaging, 3D reconstruction, cheetah skull, early Pleistocene, Tangshan, Nanjing.

The probability of fossilization and preservation of life remains is very small, and the well preserved fossils are even rare. It is therefore impossible to really dissect a rare and precious fossil specimen for anatomic studies, and the morphological study is restricted to the exterior of the specimens. In some cases, the well preserved fossils are too fragile to be prepared or cast due to the long-term soakage by underground water. These difficulties evidently limited the further research on fossil specimens. Computer tomography (CT) can solve the shadow problem of X ray clairvoyant imaging and help palaeontologists to learn some interior morphology of fossil specimens[1—4]. However, it is very abstract to understand and illustrate the interior morphology, which limits the discussion and communication inter-disciplinarily. With the development of information technology, the three-dimensional (3D) visualization technique has been improved greatly in recent years, making it possible for palaeontologists to process the CT data with 3D visualization software[5,6], reconstruct 3D virtual human fossil skull on computer and carry out virtual specimen dissection[7—11], endocranium study[12,13], occlusal function study of dinosaurs[14,15], remedy the fossil skulls distorted or broken by post-mortem compression before being excavated, and take related measurements[16,17]. Here we show a study on a virtually reconstructed 3D skull based on CT data scanned from an early Pleistocene cheetah skull unearthed from the Tuozi cave, Tangshan, Nanjing.

1 Material and methods

1.1 Material

The extant cheetah is the fastest runner of the world with the top speed of about 110 km/h. It becomes the fastest mammal thanks not only to its long limbs, flexible trunk, strong heart and large lungs, but also to its streamlined head and widely open nose for efficient breath[18]. The morphological and evolutionary study of the cheetah skull is of both biological and bionics significances. We selected a fossil cheetah skull unearthed from the early Pleistocene deposits in the Tuozi cave at Tangshan, Nanjing, Jiangsu Province of China, as material. The fauna associated with the skull includes *Hipparion*, *Equus* and *Leptobos*, its biochronological age is equivalent to European mammalian zonation MN16, or about 2.4 Ma (Million years ago)[19,20]. According to the definition

* Supported by National Natural Science Foundation of China (Grant No. 40372016) and the State Key Laboratory of Pattern Recognition, Institute of Automation, Chinese Academy of Sciences

** To whom correspondence should be addressed. E-mail: dongwei@ivpp.ac.cn

of Chinese geologists, the limit between the Pliocene and Pleistocene is defined at the boundary between Matuyama and Gauss palaeomagnetic polarity events[21], and the geological age of the Tuozi cave deposits and the fauna is of the early Pleistocene. The nostril part, both zygomatic arches and right auditory bulla of the skull are broken, but the rest parts, especially the cranium, are well preserved. Its morphology is between that of *Sivapanthera*[22] and *Acinonyx*. Judged by its more swelling cranium and more streamlined skull, its smaller skull length than that of the *Sivapanthera*, we assign the specimen into *Acinonyx*, the same genus as extant cheetah. The present paper focuses on the morphological study of the endocranium, which is impossible with conventional methods, and we will leave taxonomic and phylogenetic studies of the specimen in a separate paper. Although the *Acinonyx* skull from the Tangshan is less complete than that of *Sivapanthera* from Longdan, Gansu Province, the former is more affiliated to the extant cheetah than the latter, and it is more suitable for the phylogenetic study.

1.2 CT scan method

The original specimen was scanned along its longitudinal axis (axial position for quadruped mammals and equivalent to coronal position for biped human) with a medical CT scanner Lightspeed QX/i made by GE MEDICAL SYSTEMS installed in the Renmin Hospital of Peking University. The interslice distance was fixed at 0.25 cm, larger than 0.1 cm as previously expected due to the capacity limits of the medical scanner which was primarily designed for patients, and so the X-ray radiation and the costs were lowered down. The scanner can only scan some tens slices once and we have to increase the interslice distance for a skull with a length of 19 cm to avoid overcharge of the scanner. The scanning specifications were set as follows: X-ray tube voltage 140 kV, X-ray tube current 120 mA, every slice exposure time 2 s, convolution kernel standard, data collection diameter 25 cm. Folded table cloth was placeed under the skull to make its position more horizontal and within the scanning field.

1.3 CT data processing method

The primary scanned slice data were processed with the two-dimensional reconstruction software LightSpeedApps (version 10.5_2.8.2I_H1.3M4) equipped with the scanner by the scanner manufacturer according to 1.1 Routine Head protocol. The complete set of slice data were saved on a CD ROM with slice pixel matrix of 512×512 and colour depth of 16 bits. The reconstruction diameter of each slice is 15.3 cm (Fig. 1(a)—(d)), each pixel size is 0.0298828 cm×0.0298828 cm. We used a 3D visualizing software Amira (Version 3.1.1) by Mercury (www.mc.com/tgs) for three processes with the CT data of the cheetah skull on the CD ROM.

1.3.1 Extraction of isosurface This process is the primary reconstruction of the 3D virtual images based on 2D slice images scanned from the specimen. The 2D slice images are the indications of the amount of X-ray penetrated through the specimen, i.e. when the amount of X-ray penetrating through the material is small, the 2D image will appear light, and the higher the density of the material, the lighter the image; on the contrary, when the amount of X-ray penetrating through the material is large, the image will appear dark, and the smaller the density of the material, the darker the image. As to the specimens from cave deposits, the density of the fossil bone is higher, and that of the matrix and filling materials (principally clay) is lower. The first step of 3D reconstruction is to line up the pixels with the same colour depth (actually the same density of materiel) to form vectorial isolines on each slice, and the second step is to associate the isolines with the same colour depth on adjacent slices to form a 3D vectorial isosurface (actually the isodensity surface). The outmost 3D isosurface of the virtual specimen is therefore very close to the shape of the real specimen, and the inner 3D isosurfaces of the virtual specimen indicate the interior morphology of the real specimen that we cannot see directly with our naked eyes. Because the reconstructed virtual specimen is just computer images, we can use them for non-invasive dissection axially, coronally, sagittaly, or at any oblique direction as we like.

1.3.2 Image segmentation The reconstructed 3D virtual specimen based on colour depth can distinguish different parts inside the specimen by different isosurfaces, but all isosurfaces based on the same colour depth are generated also in the same colour on computer. Therefore, it is necessary to segment the different structures, tissues, or organs if we want to distinguish them clearly. This work can only be done by morphologists of the specimens. The first step of segmentation is to define the boundaries of related organs or structures on the 2D slices with different colours for different organs by using automatic selec-

tion tool for quick and brief definition, and the second step is manual selection to confirm or revise incorrect boundaries defined in the first step slice by slice. The software can then extract the 3D organs segmented with different colours on computer based on defined boundaries. The image segmentation is the key process for virtual anatomy, and it is the hardest and most precise work in the project.

Due to the interslice distance and bimap format of 2D slice, the isolines and isosurfaces generated are usually scalariform. To avoid such discrepancy between the virtual and real morphology of the specimen, a smoothing function was used to moderate scalariform surfaces so that the virtual specimen can appear as close to the original one as possible.

1.3.3 Specimen measurements Reconstructed and extracted virtual images are all based on CT slice images which are of bimap format. The bimap CT slice image is composed of a matrix of pixels with the same size but with different colour depths corresponding to different material densities, and every pixel corresponds to a real area; the reconstructed 3D bimap image is composed of a cubic matrix of voxels with the same volume but with different colour depths corresponding to different material densities, and every voxel also corresponds to a real volume. The real area of every pixel in our CT images measures 0.0298828 cm × 0.0298828 cm, and the real volume of every voxel in the reconstructed 3D virtual specimen measures 0.0298828 cm × 0.0298828 cm × 0.25 cm. Therefore, it is possible to calculate the dimensions, areas and volumes of different parts of the virtual specimen based on the numbers of the contained pixels and voxels. That is to say, the distance between any two voxels can be calculated by the trigonometric function according to their voxel coordinates in the cubic matrix; the area of any geometric plan can be calculated according to the number of pixels the plan contained and the area of every pixel; the volume of any geometric object can be calculated according to the number of voxels the object contained and the volume of every voxel.

2 Reconstruction and anatomy of virtual 3D skull

We scanned the fossil cheetah skull from the early Pleistocene deposits in the Tuozi cave with the above mentioned method and obtained 76 slices of CT images. We can see from the slice images that although there are some uneven fillings inside the skull, some soft tissues such as cerebral falx are not preserved, the main structure of the cranium such as positions and outlines of cerebral fossa, cerebella fossa, olfactory fossa, and frontal sinus, etc., are quite clear on the slices (Fig. 1 (a)—(d)), and they can be segmented and extracted. We segmented and extracted them (Fig. 1 (e)—(f), Fig. 2), reconstructed virtually dissectible 3D skull (Fig. 1 (e)—(f), Fig. 2(c)1), and took the measurements of every part of the endocranium (Table 1).

Table 1. Measurements of virtual skull of the early Pleistocene cheetah from the Tuozi cave, Tangshan, Nanjing

Material	Voxel count[a)]	Volume (mL)	Center X	Center Y	Center Z
Skull	19007060	4243.24	7.59888	7.67473	9.56815
Cerebellar fossa	131080	29.26	8.31858	7.82084	2.59109
Cerebral fossa	615060	137.31	8.43288	6.31446	5.98383
Olfactory fossa	12639	2.82	8.47451	7.34700	10.37548
Medullary fossa	108228	24.16	8.21787	9.57672	3.47958
Frontal sinus	48878	10.91	8.32082	4.10175	7.92605

a) Voxel size: 0.0298828 cm × 0.0298828 cm × 0.25 cm

We observed and compared the virtual skull and endocranium of the Tuozi cave cheetah by referring to the cranial and brain anatomy of the domestic cat[23], giant panda[24], domestic dog, pig, cattle and horse[25], as well as gibbon[26]. The endocerebrum of the Tuozi cave cheetah is anteriorly narrow and posteriorly wide, close to a triangle, in dorsal view (Fig. 1 (f), Fig. 2 (b)); it is superiorly large and inferiorly small, posteriorly large and anteriorly small in lateral view (Fig. 1 (e)). Its shape is similar to that of domestic cat and dog. However, its sulcus and gyrus indicated by the endocranium are more complicated than those of the domestic cat but similar to those of the domestic dog, and simpler than those of the giant panda, domestic pig, cattle and horse. This phenomenon is very likely related to the volume of the brain, because based on our analyses on the brain data of many different mammals[27], the brain with larger

volume tends to have more sulcus and gyrus, and the size of the cheetah brain is larger than that of domestic cat, slightly larger than that of domestic dog, but evidently smaller than that of giant panda, pig, cattle and horse. Some of the sulcus and gyrus on the endocranium of the Tuozi cave cheetah are quite distinguishable as that in Fig. 2(b), but others are not so distinguishable. It is due to the quality of the fossil preservation and the resolution of CT scanner on the one hand, and the endocranium is just the indication of the bony structure contacting and containing the brain instead of the brain itself on the other hand.

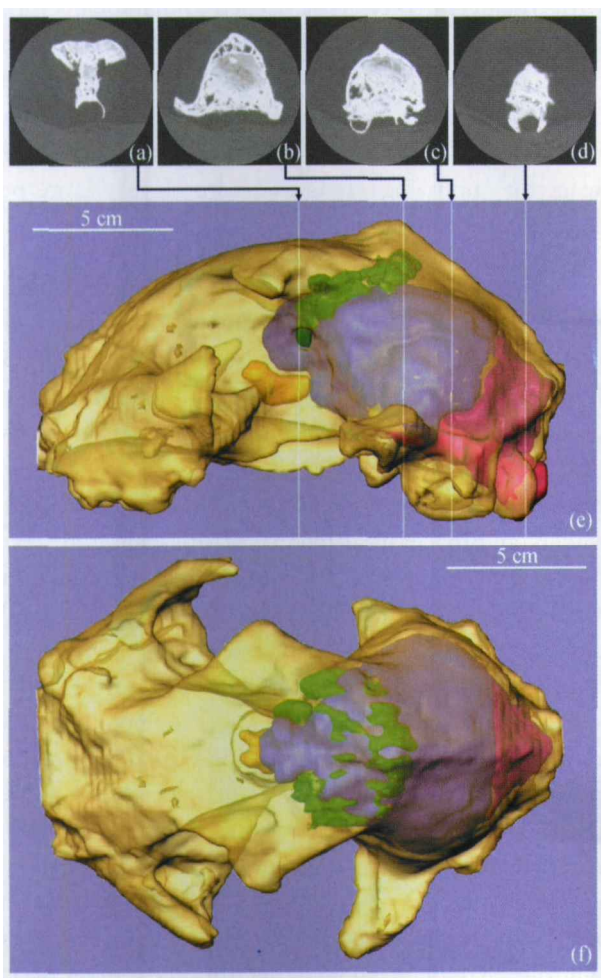

Fig. 1. Reconstructed 3D virtual skull and endocranium of fossil cheetah based on CT data. (a)—(d) Representative CT slices (slice size: 15.3 cm×15.3 cm); (e) left view of virtual endocranium and its position in transparent skull, as well as the positions of representative CT slices on the skull; (f) dorsal view of virtual endocranium and its position in transparent skull.

The CT data show that the frontal sinus of the fossil cheetah is somewhat beehive-like (Fig. 1(e)—(f); Fig. 2(a)) instead of being a whole sinus. It takes a volume of 10.91 mL in the frontal (Table 1). Such a structure can reduce the weight of the skull

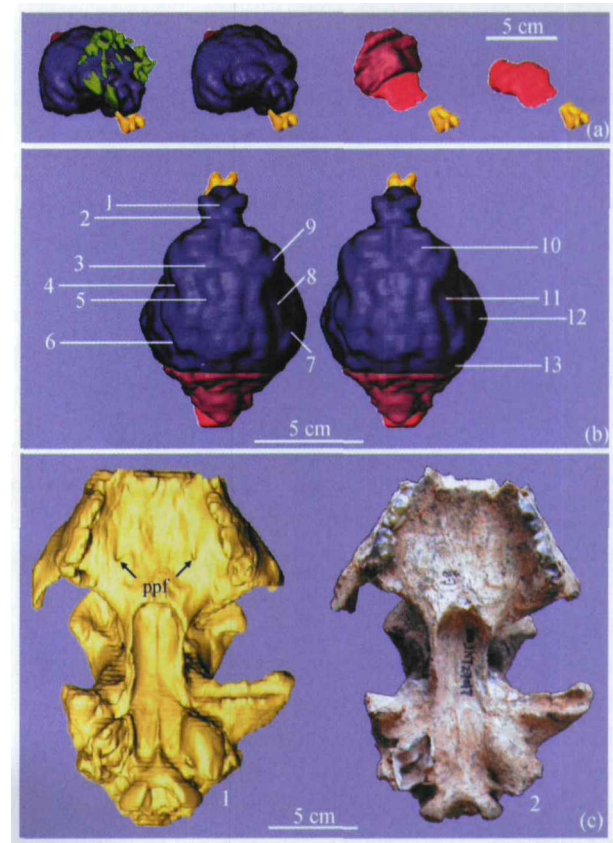

Fig. 2. Fossil cheetah skull and its endocranium. (a) Endocranium series of fossil cheetah: frontal sinus (green), cerebral fossa (blue), cerebellar fossa (purple), olfactory fossa (orange) and medullary fossa (pink); (b) dorsal stereoimages of the endobrain: 1. longitudinal fissure, 2. precruciate sulcus, 3. cruciate sulcus, 4. coronal sulcus, 5. postcruciate sulcus, 6. sylvius sulcus, 7. sylvius gyrus, 8. coronal gyrus, 9. sigmoid gyrus, 10. frontal lobe, 11. parietal lobe, 12. temporal lobe, 13. occipital lobe; (c) ventral view of fossil cheetah skull: 1. virtual specimen (ppf: postpalatine foramen), 2. real specimen.

without losing the intensity of the skull, and we interpret it as an adaptation to the hunting and fighting life style of cheetah. The virtual endocranium (Fig. 2(b)) shows that the frontal lobe (locomotion area) anterior to the coronal sulcus and postcruciate sulcus is relatively large, the body length of extant cheetah is similar to that of domestic pig, but the proportion of the frontal lobe to the cerebrum is obviously smaller in domestic pig than in fossil cheetah; the parietal lobe (body sense area) posterior to the coronal sulcus and anterior to the sylvius sulcus is moderate, the same is for the occipital lobe (visual area) in the posterior part of cerebrum; the temporal lobe (auditory area) between the sylvius sulcus and postmarginal sulcus is relatively small. It probably implies that the locomotive function of the fossil cheetah from the Tuozi cave is relatively strong but its auditory function is relatively weak. The body mass and the whole size of the cheetah are both close to those of *Homo*

erectus, but the cranium volume of the fossil cheetah from the Tuozi cave measures 193.55 mL, smaller than one fifth of that of the Peking Man (average 1075 mL)[28]. This comparison shows that the brain volume of the Tuozi cave cheetah is quite small, and the cerebral sulcus and gyrus are not well developed. It implies that the intelligence of the fossil cheetah is not high, but its cerebella is relatively large, which means that its equilibrium and locomotion abilities are strong, in addition to its relatively large frontal lobe. We interpret that the fossil cheetah from the Tuozi cave could already run very fast.

The virtual skull of the fossil cheetah from the Tuozi cave also shows some morphological structures unclear from the real specimen. As shown in Fig. 2 (c), the postpalatine foramens (ppf) are quite clear on the virtual skull, but they are not evident on the real specimen. The foramens are filled with matrix in real specimen before being unearthed. But the matrix has different densities from that of the fossil bone and the matrix is automatically neglected during reconstruction of the isosurfaces of the virtual skull. The postpalatine foramens are located on the midline of two upper third premolars, similar to those of *Sivapanthera linxiaensis* from the Linxia, Gansu Province[22].

3 Discussion

The quality of reconstructed 3D virtual specimens depends on three main factors: the preservation quality of fossil specimens itself, the resolution of CT scanner and the power of CT data processing tools (e.g. speed and capacity of both hardware and software). It is no longer a problem if the fossil specimens are distorted in the deposits because the distortion can be virtually remedied. But when fossil bones are mineralized with the matrix and filling that have the similar or even the same density, it will be very hard to distinguish bones from matrix and fillings on CT slices. There are many kinds of CT scanners nowadays. The medical CT scanners have less varieties but are very numerous and installed in many large hospitals. They are mainly designed for diagnosing human body, they work well when the specimens are close to human size and scanning interslice distance is not required to be very small. The present work was carried out with a medical scanner and it fitted the requirements of the study on endocranial morphology. The industrial CT scanners have more varieties but are less numerous. Their scanning resolution can be configured very high, the interslice distance can also be configured very small, so that more information can be scanned into the CT data and the precision of the CT images can be improved. However, very long scanning time is needed. Therefore, different specimens with different sizes need different kinds of scanners. The famous skull of *Sahelanthropus* from Chad was scanned with an interslice of 0.04 cm, and tube voltage as high as 450 kV[17]. The whole scanning process took two days and the CT data are very large. It is evident that a rapid and powerful computer with large memory and equipped with intelligent software is needed to manipulate large CT data set. Among the three factors mentioned above, the preservation quality of the fossil specimens is unchangeable, but the resolution of CT scanner and the power of data processing tools still have large space for improving. It is therefore of very large potential for development.

The application of the virtual 3D imaging technique in palaeontology is a great breakthrough in methodology. First of all, it extends the study on fossil specimens from the exterior to the interior (e.g. observation of endocranium, embryos inside eggs, etc.), and that will help us to find more unknown characteristics inside the fossil specimens and to better understand the natural history of life evolution. Secondly, it is often a pity that although the fossils are well preserved in the deposits, they are too fragile and weather-prone to be prepared or conserved for long-term (e.g. the mammal specimens from Shanwang diatom shales in Shangdong Province). We can now solve such a problem with the virtual 3D imaging technique, e.g. we can leave such specimens unprepared but strengthen them directly with chemical compounds to prevent weathering, and then scan the specimens and virtually remove the matrix from the reconstructed 3D specimens for detailed studies. Thirdly, it is well known that the mysterious disappearance of the Peking Man skulls from the Zhoukoudian during World War II is a great loss for palaeontology. Although humankind can strive to avoid wars, the uncontrollable factors such as earthquakes, fires, terrorist attacks and natural weathering, etc., still menace the conservation of rare and precious fossil specimens. If we get CT data from all such specimens, we can conserve both exterior and interior morphology of the specimens permanently, and we can use stereolithographical modeling machine to reproduce the casts of such specimens at any time

with the virtual 3D specimen data[7]. Lastly, judged by the developing situation of information technology, the function, speed and prices of computer and internet can be suitable enough in a decade for palaeontologists to easily transfer data of virtual 3D specimens for communication and discussion; experts and university students can also visit the virtual museum and study the virtual 3D specimens. Therefore, the application of this technique to palaeontology has great foreseeable prospect.

Acknowledgement The authors would like to thank Mercury (www. mc. com/tgs) for supplying 3D visualizing software Amira.

References

1 Eubanks B. A., Cann C. E. and Brand-Zawadski M. CT measurement of the diameter of spinal and other bony canals: effects of section angle and thickness. Radiology, 1985, 157: 243—246.
2 Conroy G. C. Enamel thickness in South African Australopithecines: noninvasive evaluation by computed tomography. Palaeont. Afr., 1991, 28: 53—59.
3 Rae T. C. and Koppe T. Isometric scaling of maxillary sinus volume in hominoids. J. Hum. Evol., 2000, 38: 411—423.
4 Weber G. W., Kim J., Neumaier A. et al. Thickness mapping of the occipital bone on CT-data—a new approach applied on OH 9. Acta Anthrop. Sin., 2000, 19(Suppl): 52—61.
5 Ketcham R. A. and Carlson W. D. Acquisition, optimization and interpretation of X-ray computed tomographic imagery: applications to the geosciences. Computers & Geosciences, 2001, 27: 381—400.
6 Dong W., Liu J. Y., Jaeger M. et al. Reconstruction and remedy of virtual 3d images of fossils. In: Proceedings of the Ninth Annual Symposium of the Chinese Society of Vertebrate Paleontology (in Chinese). Nanning, 2004. Beijing: China Ocean Press, 2004, 175—182.
7 Seidler H., Falk D., Stringer C. et al. A comparative study of stereolithographically modelled skulls of Petralona and Broken Hill: implications for future studies of middle Pleistocene hominid evolution. J. Hum. Evol., 1997, 33: 691—703.
8 Zollikofer C. P. E. and Ponce de León M. S. Computer-assisted paleoanthropology: methods, techniques and applications. Acta Anthrop. Sin., 2000, 19(Suppl): 90—97.
9 Zollikofer C. P. E. and Ponce de León M. S. Computer-assisted morphometry of hominoid fossils: The role of morphometric maps. In: Hominid Evolution and Climatic Change in Europe. Cambridge: Cambridge University Press, 2001, 50—59.
10 Ponce de León M. S., Zollikofer C. P. E., Martin R. D. et al. Investigation of Neanderthal morphology with computer-assisted methods. In: Neanderthals at the Edge. Oxford: Oxbow Books, 2000, 237—248.
11 Ponce de León M. S. and Zollikofer C. P. E. Neanderthal cranial ontogeny and its implications for late hominid diversity. Nature, 2001, 412: 534—537.
12 Falk D., Hildebolt C., Smith K. et al. The Brain of LB1, *Homo floresiensis*. Science, 2005, 308: 242—245.
13 Weber J., Czarnetzki A. and Pusch C. M. Comments on "The Brain of LB1, *Homo floresiensis*". Science, 2005, 310: 236—236.
14 Erickson G. M. The bite of Allosaurus. Nature, 2001, 409: 987—988.
15 Rayfield E. J., Norman D. B., Horner C. C. et al. Cranial design and function in a large theropod dinosaur. Nature, 2001, 409: 1033—1037.
16 Vialet A., Li T., Grimaud-Hervé D. et al. Proposition de reconstitution du deuxième crâne d'*Homo erectus* de Yunxian (Chine). C. R. Palevol, 2005, 4(3): 265—274.
17 Zollikofer C. P. E., Ponce de León M. S., Lieberman D. E. et al. Virtual cranial reconstruction of *Sahelanthropus tchadensis*. Nature, 2005, 434: 755—759.
18 Hildebrand M. Analysis of Vertebrate Structure. New York: John Wiley & Sons, 1982, 1—654.
19 Dong W. and Fang Y. S. The Cervidae (Artiodactyla, Mammalia) from the Tuozidong at Tangshan, Jiangsu Province, China. Acta Anthrop. Sin. (in Chinese), 2004, 23(suppl): 197—206.
20 Dong W. and Fang Y. S. Fossil equids (mammals) from the Tuozidong, Nanjing (China) and its significance. Vert. PalAsiatica (in Chinese), 2005, 43(1): 36—48.
21 Liu J. Q. and Liu Q. Quaternary stratigraphy in China. Quaternary Sciences (in Chinese), 2000, 20(2): 129—141.
22 Qiu Z. X., Deng T. and Wang B. Y. Early Pleistocene Mammalian Fauna from Longdan, Dongxiang, Gansu, China. Palaeont. Sin., New Ser. C (in Chinese), 2004, (27): 1—198.
23 Lu Z. H. Anatomy of Domestic Cat (in Chinese). Beijing: Science Press, 1979, 1—155.
24 Beijing Zoo, Beijing University, Beijing Agricultural University et al. Morphology of the Giant Panda—Systematic Anatomy and Organ-History (in Chinese). Beijing: Science Press, 1986, 1—641.
25 Beijing Agriculture University, Inner Mongolian Agriculture and Pasture College. Anatomy of Domestic Animals (Part II) (in Chinese). Beijing: Agriculture Press, 1961, 1—233.
26 Gibbon Anatomy team of the Institute of Vertebrate Paleontology and Paleoanthropology and Kunming Zoology Institute of Chinese Academy of Sciences. Gibbon Anatomy (in Chinese). Beijing: Science Press, 1978, 1—163.
27 Welker W., Johnson J. I. and Noe A. Comparative mammalian brain collections. http: //www. brainmuseum. org/ [2006-2-20].
28 Wu R. K., Wu, X. Z., Huang W. W. et al. Paleolithic Sites in China (in Chinese). Shanghai: Shanghai Scientific and Technological Education Publishing House, 1999, 1—307.